Chemistry of the Vanadium–Carbon σ Bond. 2. Oxovanadium(IV) and Oxovanadium(V) Containing Metal-to-Carbon σ Bonds

Marilin Vivanco,[†] Javier Ruiz,[†] Carlo Floriani,[*,†] Angiola Chiesi-Villa,[‡] and Corrado Rizzoli[‡]

Section de Chimie, Université de Lausanne, Place du Château 3,
CH-1005 Lausanne, Switzerland, and Istituto di Strutturistica Chimica, Centro di Studio
per la Strutturistica Diffrattometrica del CNR, Università di Parma, I-43100 Parma, Italy

Received October 8, 1992

This is a report on the oxidation of organometallic vanadium(III) homoleptic compounds to the corresponding oxovanadium(V) derivatives by the use of either epoxides or molecular oxygen. Complex **1**, $[V(Mes)_3(THF)]$, gave a clean deoxygenation of epoxides with the formation of $[OV(Mes)_3]$ (**2**). The reaction of **1** with **2** to give $[\{(Mes)_3V\}(\mu_2\text{-}O)]$ (**3**) exemplifies a general method for making (μ-oxo)vanadium(IV) dimers. Complex **3** undergoes a ligand redistribution reaction in the presence of coordinating solvents and with pyridine gave $[(Mes)_2VO(py)_2]$ (**4**). Epoxides were good reagents for converting $[V\{\eta^2\text{-}C(Mes){=}NBu^t\}_3]$ (**5**) to $[OV\{\eta^2\text{-}C(Mes){=}NBu^t\}_3]$ (**6**) without affecting the V—C bond. The thermal instability and reactivity of **6** is much higher than for **2**. Reacting protic agents with **6** displaced a single iminoacyl to form $[OV\{\eta^2\text{-}C(Mes){=}NBu^t\}_2(OOCCH_3)]$ (**7**) and $[OV\{\eta^2\text{-}C(Mes){=}NBu^t\}_2(Cl)]$ (**8**) from CH_3COOH and HCl, respectively. The reaction with ethylene sulfide gave $[V\{\eta^2\text{-}C(Mes){=}NBu^t\}_2\{S{-}C(Mes){=}NBu^t\}]$ (**10**), resulting from the insertion of sulfur into one of the V—C bonds via the probable intermediacy of $[S{=}V\{\eta^2\text{-}C(Mes){=}NBu^t\}_3]$ (**9**). Complex **10** was oxidized by O_2 to the corresponding oxovanadium(V) derivative $[OV(\eta^2\text{-}C(Mes){=}NBu^t\}_2\{S{\cdots}C(Mes){\cdots}NBu^t\}]$ (**12**). The oxidation of $[V\{O{-}C(Mes){=}NR\}_3]$ (R = Ph, **13**; R = C_6H_{11}, **14**) with molecular oxygen is a clean reaction, producing $[OV\{O{-}C(Mes){=}NR\}_3]$ (R = Ph, **17**; R = C_6H_{11}, **18**) in high yield. Reaction of **17** with **13** led to the μ-oxo dimer $[(V\{O{-}C(Mes){=}NR\}_3)_2(\mu_2\text{-}O)]$ (**19**). Crystallographic details: **2** is monoclinic, space group $P2_1/c$, with a = 18.254(2) Å, b = 15.960(2) Å, c = 8.200(1) Å, $\alpha = \gamma = 90°$, β = 101.11(1)°, Z = 4, and R = 0.051; **4** is monoclinic, space group $C2/c$, with a = 13.374(1) Å, b = 10.346(1) Å, c = 21.798(2) Å, $\alpha = \gamma = 90°$, β = 98.41(1)°, Z = 4, and R = 0.058; **7** is monoclinic, space group $P2_1/n$, with a = 19.517(2) Å, b = 8.454(1) Å, c = 19.103(2) Å, $\alpha = \gamma = 90°$, β = 102.58(1)°, Z = 4, and R = 0.068; **10** is monoclinic, space group $P2_1/n$, with a = 12.970(1) Å, b = 32.080(3) Å, c = 11.120(1) Å, $\alpha = \gamma = 90°$, β = 98.58(1)°, Z = 4, and R = 0.079; **17** is monoclinic, space group $P2_1/n$, with a = 12.242(1) Å, b = 33.707(3) Å, c = 10.330(1) Å, $\alpha = \gamma = 90°$, β = 93.16(1)°, Z = 4, and R = 0.062.

Introduction

High-valent metal–oxo organometallic chemistry is an area of growing interest.[1] There are two major interests in this field: the oxo environment may mimic the organic fragments bonded on a metal–oxo matrix; the proximity of an oxo to an alkyl or aryl group may be important to the stoichiometric and catalytic oxidation of organic molecules mediated by transition metals.[2] We add that, in general, the reactivity of the M–C functionality has been well investigated in the presence of ancillary ligands other than the oxo groups.[1c]

What about the synthetic methodology leading to these compounds? The alkylation of high-oxidation-state starting materials is only rarely a successful method, because alkylating agents very often reduce the metal. On the other hand, the reaction of molecular oxygen or oxygen transfer agents with organometallic derivatives containing metal–carbon σ bonds has to date been regarded as leading to an uncontrolled degradation of the organic functionality.[3] The metal–carbon σ bond, or the carbon center, is normally the most reactive center of homoleptic organometallic derivatives. In such reactions, dioxygen or dioxygen transfer agents usually bind first to the metal but then are transferred to the organic functionality.[2] In very rare cases the direct oxidation of the metallic center by either oxygen or oxygen transfer agents leads cleanly to the corresponding oxo–alkyl or –aryl derivatives.[4]

This is the first report on well-characterized examples of oxovanadium(V) and -vanadium(IV) derivatives[5] containing V–C σ bonds. The high-yield syntheses of these compounds have been performed using dioxygen and

---

[*] To whom correspondence and reprint requests should be addressed.

[†] University of Lausanne.

[‡] University of Parma.

[1] (a) Bottomley, F.; Sutin, L. *Adv. Organomet. Chem.* 1988, *28*, 339. (b) Herrmann, W. A. *Angew. Chem., Int. Ed. Engl.* 1988, *27*, 1297. (c) Nugent, W. A.; Mayer, J. M. *Metal-Ligand Multiple Bonds*; Wiley: New York, 1988.

[2] (a) Sheldon, R. A.; Kochi, J. K. *Metal-Catalyzed Oxidations of Organic Compounds*; Academic: New York, 1981. (b) Mimoun, H. In *Comprehensive Coordination Chemistry*; Wilkinson, G., Gillard, R. D., McCleverty, J. A., Eds.; Pergamon: Oxford, U.K., 1987; Vol. 6, Chapter 61.3, p 317.

[3] Kochi, J. K. *Organometallic Mechanisms and Catalysis*; Academic: New York, 1978; p 517.

[4] For a recent report on chromium chemistry, see: Noth, S.-K.; Heintz, R. A.; Haggerty, B. S.; Rheingold, A. L.; Theopold, K. H. *J. Am. Chem. Soc.* 1992, *114*, 1892.

[5] Connelly, N. G. Vanadium. In *Comprehensive Organometallic Chemistry*; Wilkinson, G., Stone, F. G. A., Abel, E. W., Eds.; Pergamon: Oxford, U.K., 1981; Vol. 3, Chapter 647.

0276-7333/93/2312-1802$04.00/0 © 1993 American Chemical Society

Table I. Experimental Data for the X-ray Diffraction Studies on Crystalline Complexes 2, 4, 7, 10 and 17

	2	4	7	10	17
formula	$C_{27}H_{33}OV$	$C_{28}H_{32}ON_2V{\cdot}0.5C_5H_5N$	$C_{30}H_{43}O_3N_2V$	$C_{41}H_{60}SN_2V{\cdot}0.25C_6H_{14}$	$C_{48}H_{48}O_4N_3V$
cryst syst	monoclinic	monoclinic	monoclinic	monoclinic	monoclinic
space group	$P2_1/c$	$C2/c$	$P2_1/n$	$P2_1/n$	$P2_1/n$
cell params at 295 K[a]					
a, Å	18.254(2)	13.374(1)	19.517(2)	12.970(1)	12.242(1)
b, Å	15.960(2)	10.346(1)	8.454(1)	32.080(3)	33.707(3)
c, Å	8.200(1)	21.798(2)	19.103(2)	11.120(1)	10.330(1)
β, deg	101.11(1)	98.41(1)	102.58(1)	98.58(1)	93.16(1)
V, Å^3	2344.2(5)	2983.7(5)	3076.3(6)	4575.0(7)	4256.1(7)
Z	4	4	4	4	4
D_{calcd}, g cm^{-3}	1.203	1.120	1.146	1.016	1.220
mol wt	424.5	503.1	530.6	699.5	781.9
cryst dimens, mm	0.40 × 0.46 × 0.50	0.18 × 0.21 × 0.28	0.32 × 0.40 × 0.52	0.25 × 0.36 × 0.55	0.42 × 0.48 × 0.52
linear abs coeff, cm^{-1}	4.22	29.66	29.38	24.37	23.09
transmissn factor range	0.832–1.000	0.793–1.000	0.725–1.000	0.592–1.000	0.837–1.000
diffractometer	Siemens AED	Siemens AED	Siemens AED	Siemens AED	Siemens AED
diffraction geometry	equatorial	equatorial	equatorial	equatorial	equatorial
radiation	*c*	*b*	*b*	*b*	*b*
2θ range, deg	6–46	6–130	6–140	6–120	6–140
scan type	θ–2θ	θ–2θ	θ–2θ	θ–2θ	θ–2θ
scan speed, deg min^{-1}	3–12	3–12	3–12	3–12	3–12
scan width, deg	$1.20 + 0.35 \tan\theta$	$1.20 + 0.015 \tan\theta$	$1.20 + 0.015 \tan\theta$	$1.20 + 0.015 \tan\theta$	$1.20 + 0.015 \tan\theta$
rflns measd	$\pm h,k,l$	$\pm h,k,l$	$\pm h,k,l$	$\pm h,k,l$	$\pm h,k,l$
unique total data	3258	2538	5847	6810	8081
criterion for observn	2	2	2	2	2
unique obsd data	1618	1041	3963	3577	5130
no. of variables	226	158	299	396	433
overdetermn ratio	7.2	6.6	13.3	9.0	11.8
max Δ/σ on last cycle	0.01	0.1	0.1	*d*	0.2
$\Delta\rho$, e Å^{-3}	0.2	0.3	0.6	0.4	0.3
$R = \sum\lvert\Delta F\rvert/\sum\lvert F_o\rvert$	0.051	0.058	0.068	0.079	0.062
$R_G = [\sum w^{1/2}\lvert\Delta F\rvert^2/\sum w^{1/2}\lvert F_o\rvert^2]^{1/2}$	0.062	0.059	0.069	0.081	0.081
GOF $= [\sum w\lvert\Delta F\rvert^2/(N_o - N_v)]^{1/2}$	0.43	2.45	1.60	2.72	1.52

[a] Unit cell parameters were obtained by least-squares analysis of the setting angles of 25–30 carefully centered reflections from diverse regions of reciprocal space. [b] Ni-filtered Cu Kα (λ = 1.541 78 Å). [c] Nb-filtered Mo Kα (λ = 0.710 688 Å). [d] 0.1 for the nondisordered atoms and 0.5 for the disordered ones.

epoxides. Epoxides were chosen because their deoxygenation is a subject of continuous synthetic and mechanistic interest,[6] with most attention being devoted to developing procedures attractive to the synthetic organic chemist. The literature contains a handful of poorly characterized compounds, with no structural determinations. They are $[VO(Ph)(Cl)_2]$,[7] $[VO(Me)(OR)_2]$ (R = Bu^t, Bu^s, Pr^i),[8] $[VO(Cl)(Ph)(OPr^i)]$,[9] and $[VO(Ph)(OPr^i)_2]$,[9] which are very thermally labile in contrast with the only well-characterized example, namely $[VO(CH_2SiMe_3)_3]$.[10] Some of the compounds in this paper have already been communicated.[11]

Results and Discussion

Tris(mesityl)vanadium(III) reacts at room temperature with styrene oxide almost quantitatively to produce the corresponding oxovanadium(V) complex:

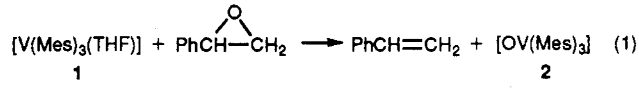

$$[V(Mes)_3(THF)] + PhCH\overset{O}{-}CH_2 \longrightarrow PhCH{=}CH_2 + [OV(Mes)_3] \quad (1)$$

1 2

Reaction 1 is surprisingly clean, and the normal oxidative degradation due to the oxidation of the metal–σ-aryl functionality is not observed. Deoxygenation of epoxides by low-valent metals is a recently explored reaction.[6] Reaction 1 has to date been used for synthetic purposes only. Some mechanistic studies involving different epoxides are in progress.[12] Complex 2 is thermally very stable, being recovered undecomposed after a long reflux in THF. The structure of 2 is reported in Figure 1, and a list of selected structural parameters in Table VII. The coordination polyhedron is a trigonal pyramid with vanadium displaced by 0.432(1) Å from the plane through the V–C σ bonds toward the oxo ligand. The V—C bond distances are significantly shorter than those in the corresponding vanadium(III).[13] The metal atom is out of the planes of the mesityl rings by 0.185(1), 0.093(1), and 0.121(1) Å. The reaction of 1 with oxygen[14a] should not be considered as a useful route to oxovanadium complexes, since it leads to the complex and to an unpredictable mixture of compounds. The formation of 2, whose characterization was rather limited, was observed in the oxidation of the proposed $[VOMes_3]^-$ with chloranil,[14b,c] a much less straightforward approach than reaction 1, which seems

---

[6] (a) Hayasi, Y.; Schwartz, J. *Inorg. Chem.* **1981**, *20*, 3473 and references therein. (b) Atagi, L. M.; Over, D. E.; McAlister, D. R.; Mayer, J. M. *J. Am. Chem. Soc.* **1991**, *113*, 870 and references therein. (c) Whinnery, L. L.; Henlung, L. M.; Bercaw, J. E. *J. Am. Chem. Soc.* **1991**, *113*, 7575 and references therein. (d) Bäckvall, J. E.; Bökman, F.; Blomberg, M. R. A. *J. Am. Chem. Soc.* **1992**, *114*, 534.

[7] Thiele, K.-H.; Schumann, W.; Wagner, S.; Brüser, W. *Z. Anorg. Allg. Chem.* **1972**, *390*, 280. Reichle, W. T.; Carrick, W. L. *J. Organomet. Chem.* **1970**, *24*, 419.

[8] Thiele, K.-H.; Adler, B.; Grahlert, H.; Lachowicz, A. *Z. Anorg. Allg. Chem.* **1974**, *403*, 279. Lachowicz, A.; Thiele, K.-H. *Z. Anorg. Allg. Chem.* **1977**, *431*, 88.

[9] Choukroun, R.; Sabo, S. *J. Organomet. Chem.* **1979**, *182*, 221.

[10] Middleton, A. R.; Wilkinson, G. *J. Chem. Soc., Dalton Trans.* **1980**, 1888. Yagupsky, G.; Mowat, W.; Shortland, A.; Wilkinson, G. *J. Chem. Soc. D* **1970**, 1369. Mowat, W.; Shortland, A.; Yagupsky, G.; Hill, N. J.; Yagupsky, M.; Wilkinson, G. *J. Chem. Soc., Dalton Trans.* **1972**, 535.

[11] Ruiz, J.; Vivanco, M.; Floriani, C.; Chiesi-Villa, A.; Guastini, C. *J. Chem. Soc., Chem. Commun.* **1991**, 762.

[12] Floriani, C.; et al., unpublished results.

[13] Vivanco, M.; Ruiz, J.; Floriani, C.; Chiesi-Villa, A.; Rizzoli, C. *Organometallics*, preceding paper in this issue.

[14] (a) Seidel, W.; Kreisel, G. *Z. Chem.* **1977**, *17*, 73. (b) **1982**, *22*, 113. (c) *Z. Anorg. Allg. Chem.* **1988**, *559*, 118.

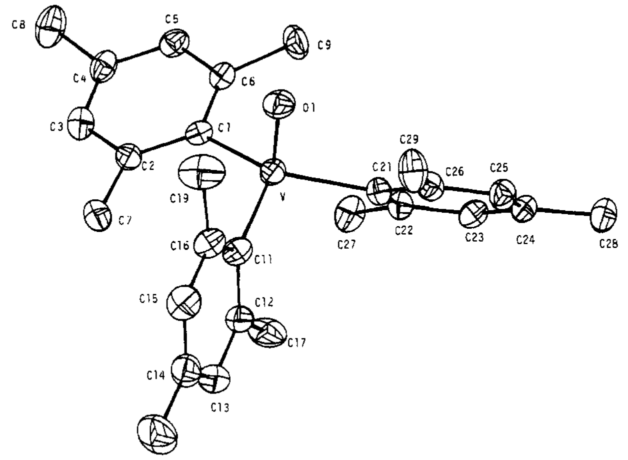

Figure 1. ORTEP view of complex **2** (30% probability ellipsoids).

the best synthetic route to oxovanadium(V) complexes. The other known example is $[OV(CH_2SiMe_3)_3]$, formed from an undefined hydrolysis and oxidation of the corresponding vanadium(IV) compound $[V(CH_2SiMe_3)_4]$.[10] The V=O bond oxidizes low-valent metals leading to μ-oxo dimetallic complexes.[14c,15] The reaction of **1** with **2** exemplifies a general reactivity pattern leading to (μ-oxo)-vanadium(IV) organometallic derivatives:

$$\underset{\mathbf{2}}{[OV(Mes)_3]} + \underset{\mathbf{1}}{[V(Mes)_3(THF)]} \xrightarrow[-THF]{toluene} \underset{\mathbf{3}}{(Mes)_3V{-}O{-}V(Mes)_3} \xrightarrow[-(Mes)_4V]{py} \underset{\mathbf{4}}{[(Mes)_2VO(py)_2]} \quad (2)$$

Complex **3** is paramagnetic with 1.65 μ_B per vanadium at 288 K. The V—O—V stretching vibration (680 cm^{-1}) is in the range expected for a μ-oxo species.

The use of polar coordinating solvents for recrystallizing **3** led to its partial or complete decomposition. The reaction with pyridine, however, led us to understand the decomposition pathway, and **4** was isolated from a ligand redistribution reaction. The μ-oxo derivatives of vanadium(IV) are very rare, because of the high stability of the terminal oxovanadium(IV).[16] Complex **4** is the only known example of an oxovanadium(IV) organometallic compound, and it has been characterized by X-ray analysis (Figure 2). A list of selected structural parameters is given in Table VIII. Complex **4** has a crystallographic C_2 symmetry. The equatorial plane of the trigonal bipyramid is defined by the two mesityl groups and the oxo ligand, while pyridines are in the axial positions. The V—C bond distances are significantly longer than in **1** and **2**.[17] Although an extended exploration into the reactivity of **2** and **4** has not yet been carried out, we observed an almost complete lack of reactivity in insertion reactions and in the reaction with protic substances. This is in sharp contrast to the chemistry of **6**. We can speculate that strongly π-donating oxo ligands stabilize high oxidation states and make the M–C bond much less polar.[1c] That epoxides are suitable oxygen transfer agents to d^2 carbenoid metals is illustrated by the reaction of the tris(iminoacyl) species (eq 3).[13]

Table II. Fractional Atomic Coordinates (×10⁴) for Complex 2

atom	*x/a*	*y/b*	*z/c*	U_{eq},[a] Å²
V	2588.6(6)	4591.1(7)	2578.7(14)	422(4)
O1	2806(2)	4671(3)	4527(5)	582(18)
C1	1805(2)	3637(2)	2398(5)	426(22)
C2	1934(2)	2826(2)	1885(5)	435(25)
C3	1409(2)	2197(2)	1945(5)	499(26)
C4	755(2)	2379(2)	2518(5)	506(28)
C5	626(2)	3189(2)	3032(5)	490(25)
C6	1151(2)	3819(2)	2972(5)	478(24)
C7	2631(4)	2547(4)	1320(9)	601(29)
C8	195(4)	1684(5)	2703(10)	776(37)
C9	1004(4)	4653(4)	3714(10)	671(28)
C11	3557(2)	4302(3)	1851(5)	471(25)
C12	3512(2)	4341(3)	135(5)	501(27)
C13	4127(2)	4121(3)	–552(5)	633(31)
C14	4788(2)	3863(3)	477(5)	671(33)
C15	4834(2)	3824(3)	2193(5)	684(33)
C16	4218(2)	4044(3)	2880(5)	533(27)
C17	2822(4)	4592(5)	–1060(8)	691(30)
C18	5429(5)	3610(6)	–283(13)	1055(44)
C19	4307(4)	3945(6)	4728(9)	879(36)
C21	2297(2)	5813(2)	1858(5)	421(23)
C22	1652(2)	6000(2)	700(5)	444(25)
C23	1455(2)	6833(2)	330(5)	493(25)
C24	1903(2)	7479(2)	1118(5)	530(25)
C25	2547(2)	7292(2)	2276(5)	530(26)
C26	2745(2)	6460(2)	2647(5)	481(27)
C27	1143(4)	5351(4)	–243(8)	600(26)
C28	1674(4)	8391(4)	766(9)	687(30)
C29	3441(4)	6329(4)	3910(10)	737(34)

[a] U_{eq} is in the form $^1/_3\sum_i\sum_j U_{ij}a_i^*a_j^*\mathbf{a}_i\mathbf{a}_j$.

Table III. Fractional Atomic Coordinates (×10⁴) for Complex 4

atom	*x/a*	*y/b*	*z/c*	U_{eq},[a] Å²
V	5000(-)	1719.9(20)	7500(-)	666(7)
O1	5000(-)	3260(7)	7500(-)	808(29)
N1	3461(4)	1588(6)	7720(3)	741(23)
C1	4514(5)	909(8)	6602(3)	686(29)
C2	4835(5)	–307(7)	6421(3)	660(28)
C3	4493(5)	–832(7)	5832(3)	760(29)
C4	3815(6)	–165(9)	5409(3)	843(36)
C5	3491(6)	1038(10)	5580(4)	934(39)
C6	3813(5)	1580(8)	6163(3)	798(31)
C7	5603(6)	–1103(7)	6826(3)	844(31)
C8	3423(7)	–742(9)	4775(4)	1087(41)
C9	3375(7)	2866(9)	6295(4)	1067(41)
C12	2704(6)	833(8)	7430(4)	838(36)
C13	1770(6)	753(10)	7623(5)	1068(45)
C14	1593(7)	1547(13)	8114(6)	1220(56)
C15	2321(7)	2332(11)	8389(4)	1046(43)
C16	3266(5)	2344(8)	8198(3)	859(32)
C1S[b]	366(31)	751(36)	–413(20)	2298(142)
C2S	542(24)	742(36)	181(20)	2119(125)
C3S	–562(32)	365(45)	–539(17)	2482(157)

[a] U_{eq} is in the form $^1/_3\sum_i\sum_j U_{ij}a_i^*a_j^*\mathbf{a}_i\mathbf{a}_j$. [b] The site occupation factors for C1S, C2S, and C3S atoms are 0.5. For these atoms the isotropic *U* values are quoted.

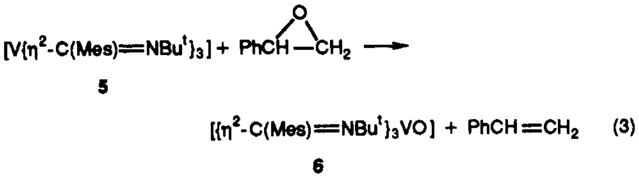

$$\underset{\mathbf{5}}{[V\{\eta^2\text{-}C(Mes){=}NBu^t\}_3]} + PhCH{-}CH_2(O) \longrightarrow \underset{\mathbf{6}}{[\{\eta^2\text{-}C(Mes){=}NBu^t\}_3VO]} + PhCH{=}CH_2 \quad (3)$$

Complex **6** is diamagnetic and monomeric in benzene. The oxidation with molecular oxygen is a complex reaction leading, as reported in part 1,[13] to the insertion of oxygen

---

(15) Young-Chiou, H.; Ladd, J. A.; Goedken, V. L. *J. Coord. Chem.* **1988**, *18*, 317, 235. Young-Chiou, H.; Goedken, V. L. *Inorg. Chim. Acta* **1986**, *117*, L19.

(16) Vilas Boas, L.; Costa Pessoa, J. *Vanadium.* In *Comprehensive Coordination Chemistry*; Wilkinson, G., Gillard, R. D., McCleverty, J. A., Eds.; Pergamon: Oxford, U.K., 1987; Vol. 3, Chapter 33.

(17) For the trans influence of the multiply bonded oxo group, see: Reference 1c, p 156.

Table IV. Fractional Atomic Coordinates (×10⁴) for Complex 7

atom	*x*/*a*	*y*/*b*	*z*/*c*	U_{eq},[a] Å²
V	−133.7(4)	2760.5(9)	1840.0(4)	467(2)
O1	−94(2)	4266(4)	2350(2)	624(13)
O2	−320(2)	3696(4)	827(2)	684(13)
O3	−281(2)	1117(4)	804(2)	667(14)
N1	−1148(2)	2053(4)	1768(2)	541(14)
N2	896(2)	2304(5)	1853(2)	566(15)
C1	−817(1)	1(3)	2751(1)	468(14)
C2	−885(1)	−1577(3)	2533(1)	502(15)
C3	−826(1)	−2778(3)	3044(1)	559(17)
C4	−701(1)	−2402(3)	3771(1)	597(19)
C5	−633(1)	−823(3)	3989(1)	631(18)
C6	−692(1)	378(3)	3479(1)	562(18)
C7	−1024(3)	−2036(6)	1758(3)	678(20)
C8	−610(4)	−3710(8)	4322(3)	926(29)
C9	−607(4)	2084(7)	3718(3)	818(26)
C10	−765(2)	1269(5)	2245(2)	456(15)
C11	−1917(2)	2205(7)	1482(3)	768(24)
C12	−2080(3)	3963(9)	1484(5)	1197(37)
C13	−2306(3)	1233(11)	1934(5)	1389(43)
C14	−2077(3)	1605(10)	719(4)	1195(33)
C21	1057(2)	645(3)	2987(1)	524(16)
C22	1026(2)	−1001(3)	2937(1)	546(18)
C23	1252(2)	−1925(3)	3549(1)	678(20)
C24	1509(2)	−1203(3)	4211(1)	780(22)
C25	1540(2)	442(3)	4261(1)	792(24)
C26	1314(2)	1367(3)	3649(1)	678(22)
C27	777(3)	−1800(6)	2226(3)	689(21)
C28	1753(4)	−2197(10)	4879(3)	1146(32)
C29	1346(4)	3156(8)	3717(3)	966(30)
C30	736(2)	1605(5)	2370(3)	512(16)
C31	1553(3)	2515(7)	1584(3)	751(22)
C32A[b]	1756(7)	4270(16)	1707(8)	815(42)
C33A	2070(8)	1254(21)	1825(9)	1113(60)
C34A	1297(8)	2224(19)	704(8)	969(51)
C32B	1573(8)	1209(21)	1053(9)	1145(59)
C33B	2206(6)	2053(16)	2239(7)	836(43)
C34B	1560(8)	4206(19)	1314(1)	1044(51)
C35	−334(3)	2414(7)	477(3)	674(21)
C36	−441(4)	2473(8)	−317(3)	1027(29)

[a] U_{eq} is in the form $^1/_3\sum_i\sum_j U_{ij}a_i^*a_j^*\mathbf{a}_i\mathbf{a}_j$. [b] The site occupation factors for the disordered C32, C33, and C34 atoms are 0.50. For these atoms the isotropic U values are quoted.

Table V. Fractional Atomic Coordinates (×10⁴) for Complex 10

atom	*x*/*a*	*y*/*b*	*z*/*c*	U_{eq},[a] Å²
V	496.2(10)	1550.9(4)	2390.8(12)	523(4)
S1	1981(2)	2034(1)	2839(2)	703(8)
N1	1834(5)	1254(2)	3233(6)	562(21)
N2	−8(5)	1668(2)	622(5)	588(25)
N3	−513(5)	1787(2)	3423(6)	621(27)
C1	3453(3)	1592(2)	4373(5)	641(33)
C2	3420(3)	1615(2)	5620(5)	720(35)
C3	4345(3)	1625(2)	6440(5)	791(35)
C4	5303(3)	1612(2)	6014(5)	887(42)
C5	5336(3)	1589(2)	4768(5)	867(43)
C6	4412(3)	1579(2)	3947(5)	751(33)
C7	2397(7)	1671(3)	6106(8)	905(43)
C8	6321(8)	1625(4)	6893(11)	1351(62)
C9	4477(7)	1607(3)	2618(9)	923(42)
C10	2447(5)	1571(2)	3517(7)	570(28)
C11	2112(6)	800(2)	3487(8)	633(32)
C12	1110(8)	553(3)	3066(10)	993(45)
C13	2469(8)	697(3)	4807(9)	877(41)
C14	2912(9)	674(3)	2709(11)	1091(50)
C21	712(4)	1022(1)	−255(4)	595(29)
C22	1675(4)	1046(1)	−667(4)	653(33)
C23	1971(4)	735(1)	−1423(4)	763(38)
C24	1305(4)	400(1)	−1767(4)	769(38)
C25	342(4)	377(1)	−1355(4)	738(34)
C26	46(4)	688(1)	−599(4)	645(31)
C27	2446(7)	1392(3)	−248(9)	891(43)
C28	1647(10)	60(3)	−2579(10)	1195(57)
C29	−988(7)	647(3)	−148(9)	875(38)
C30	433(6)	1323(2)	671(7)	529(30)
C31	−442(8)	1959(3)	−409(8)	807(39)
C32A[b]	−1076(20)	1698(6)	−1471(19)	791(73)
C33A	498(21)	2163(9)	−941(26)	1158(103)
C34A	−1019(19)	2293(8)	80(21)	920(88)
C32B	−1627(17)	2071(7)	−165(18)	1026(78)
C33B	230(17)	2362(7)	−174(21)	1098(86)
C34B	−442(19)	1759(6)	−1656(19)	967(73)
C41	−1587(4)	1152(2)	3691(6)	652(32)
C42	−2517(4)	1092(2)	2902(6)	762(40)
C43	−3295(4)	839(2)	3250(6)	1036(49)
C44	−3144(4)	646(2)	4387(6)	1121(62)
C45	−2214(4)	706(2)	5176(6)	987(46)
C46	−1436(4)	959(2)	4828(6)	798(40)
C47	−2694(7)	1282(4)	1664(10)	1017(47)
C48	−4043(9)	394(4)	4752(15)	1627(77)
C49	−433(8)	997(3)	5669(9)	970(45)
C50	−752(6)	1403(2)	3256(8)	625(33)
C51	−963(8)	2144(3)	4058(10)	934(43)
C52A	−1060(19)	2515(7)	3280(21)	1008(77)
C53A	−8(18)	2262(7)	5234(21)	1088(88)
C54A	−1872(17)	2009(7)	4754(20)	993(79)
C52B	−2142(19)	2210(7)	3285(21)	1142(92)
C53B	−966(20)	2053(7)	5388(23)	1176(92)
C54B	−332(18)	2540(7)	3820(20)	954(75)
C1S	491(66)	4639(27)	4083(77)	2359(486)
C2S	−2(48)	4886(17)	4546(45)	2849(249)
C3S	414(42)	4428(18)	3483(52)	2993(259)

[a] U_{eq} is in the form $^1/_3\sum_i\sum_j U_{ij}a_i^*a_j^*\mathbf{a}_i\mathbf{a}_j$. [b] The site occupation factors are 0.45 and 0.55 for the A and B positions of C32, C33, and C34 and 0.5 for C52, C53, C54, C1S, C2S, and C3S. For these atoms the isotropic U values are quoted.

into the V—C bond and producing isocyanate derivatives. Unlike **2**, complex **6** does not react with its precursor **5**.

In the ^{1}H NMR spectrum, the three iminoacyl groups are equivalent at 20 °C, while at −40 °C only two of them are equivalent, with unequivalent *o*-methyl groups at the mesityl substituent. The third mesityl has a free rotation around the Mes–CNBu^t bond. Such a finding may suggest a multiple interaction of two iminoacyls in the equatorial plane (shown by A) of a bipyramidal geometry, where the axial positions are filled by the oxo and the third iminoacyl ligand. The nonequivalence of the methyl groups may be due to the interaction with the metal.

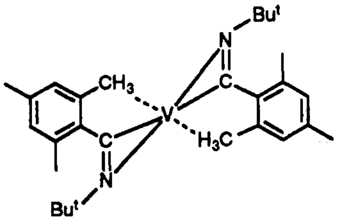

A

The structure A should account for the nonequivalence of the iminoacyl groups and the *o*-methyls on two mesityl substituents. The oxo complex **6** is thermally labile, and it has to be handled at 0 °C or lower temperature. In contrast with **2**, the V–C bond is very easily cleaved by protic species, as reported in reaction 4 for CH_3COOH and HCl.

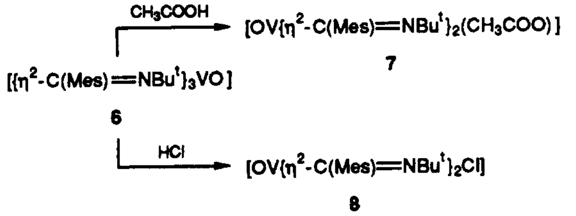

$$\underset{\mathbf{6}}{[(\eta^2\text{-C(Mes)=NBu}^t)_3\text{VO}]} \xrightarrow{\text{CH}_3\text{COOH}} \underset{\mathbf{7}}{[\text{OV}(\eta^2\text{-C(Mes)=NBu}^t)_2(\text{CH}_3\text{COO})]} \qquad (4)$$

$$\underset{\mathbf{6}}{[(\eta^2\text{-C(Mes)=NBu}^t)_3\text{VO}]} \xrightarrow{\text{HCl}} \underset{\mathbf{8}}{[\text{OV}(\eta^2\text{-C(Mes)=NBu}^t)_2\text{Cl}]} \qquad (5)$$

Both compounds **7** and **8** were isolated in high yield, and the protonolysis is selective for the first iminoacyl.

Table VI. Fractional Atomic Coordinates (×10⁴) for Complex 17

atom	x/a	y/b	z/c	U_{eq},[a] Å^2
V	8538.8(5)	1042.9(2)	6739.2(7)	505(2)
O1	8963(2)	1418(1)	5158(3)	620(10)
O2	9238(2)	842(1)	8420(3)	558(9)
O3	7954(2)	1577(1)	7704(3)	623(11)
O4	8681(2)	672(1)	5807(3)	661(11)
N1	10051(2)	1308(1)	6823(3)	571(12)
N2	7551(2)	716(1)	7970(3)	585(12)
N3	7050(2)	1270(1)	6142(3)	555(11)
C1	10788(2)	1680(1)	4985(2)	520(14)
C2	11312(2)	1484(1)	4005(2)	542(14)
C3	12141(2)	1674(1)	3369(2)	625(15)
C4	12446(2)	2061(1)	3714(2)	696(18)
C5	11921(2)	2257(1)	4694(2)	739(19)
C6	11092(2)	2067(1)	5329(2)	631(16)
C7	11019(4)	1064(2)	3643(5)	802(20)
C8	13343(4)	2263(2)	3034(6)	1045(26)
C9	10511(5)	2285(2)	6366(5)	1020(25)
C10	9933(3)	1470(1)	5667(4)	535(14)
C11	10961(2)	1342(1)	7707(2)	525(13)
C12	10782(2)	1496(1)	8930(2)	676(16)
C13	11651(2)	1532(1)	9855(2)	895(22)
C14	12699(2)	1414(1)	9555(2)	969(25)
C15	12879(2)	1260(1)	8332(2)	831(21)
C16	12009(2)	1224(1)	7407(2)	625(14)
C21	8436(2)	437(1)	10033(2)	489(12)
C22	8488(2)	645(1)	11202(2)	515(14)
C23	8583(2)	439(1)	12376(2)	562(14)
C24	8627(2)	26(1)	12380(2)	571(13)
C25	8575(2)	−182(1)	11211(2)	579(15)
C26	8480(2)	23(1)	10038(2)	513(13)
C27	8458(4)	1096(1)	11206(5)	761(18)
C28	8726(4)	−191(1)	13647(4)	797(21)
C29	8435(4)	−211(1)	8780(4)	717(16)
C30	8361(3)	663(1)	8793(4)	514(14)
C31	6492(2)	547(1)	8020(3)	582(14)
C32	6068(2)	337(1)	6941(3)	816(20)
C33	5027(2)	170(1)	6950(3)	1073(26)
C34	4410(2)	211(1)	8038(3)	1042(26)
C35	4835(2)	420(1)	9117(3)	902(22)
C36	5876(2)	588(1)	9108(3)	691(18)
C41	6289(2)	1906(1)	6939(3)	595(15)
C42	6173(2)	2172(1)	5904(3)	726(16)
C43	5402(2)	2476(1)	5926(3)	787(19)
C44	4749(2)	2515(1)	6982(3)	778(20)
C45	4865(2)	2250(1)	8017(3)	725(17)
C46	5636(2)	1946(1)	7996(3)	625(15)
C47	6878(5)	2147(2)	4773(5)	987(24)
C48	3945(5)	2852(2)	7025(6)	1127(28)
C49	5760(4)	1672(1)	9139(5)	757(19)
C50	7102(3)	1576(1)	6937(4)	558(14)
C51	6203(2)	1174(1)	5212(3)	584(15)
C52	6498(2)	1037(1)	4005(3)	870(22)
C53	5692(2)	924(1)	3072(3)	1170(28)
C54	4590(2)	946(1)	3346(3)	1123(30)
C55	4295(2)	1083(1)	4553(3)	993(24)
C56	5102(2)	1197(1)	5486(3)	739(17)

[a] U_{eq} is in the form $^1/_3\sum_i\sum_j U_{ij}a_i^*a_j^*\mathbf{a}_i\mathbf{a}_j$.

Table VII. Selected Bond Distances (Å) and Angles (deg) for Complex 2

V–O1	1.575(4)	V–C11	2.025(4)
V–C1	2.075(4)	V–C21	2.077(3)
C11–V–C21	108.7(2)	V–C1–C6	116.5(2)
C1–V–C21	122.2(1)	V–C1–C2	123.3(3)
C1–V–C11	116.1(2)	V–C11–C16	126.3(3)
O1–V–C21	102.3(2)	V–C11–C12	113.7(3)
O1–V–C11	104.7(2)	V–C21–C26	117.9(3)
O1–V–C1	99.6(2)	V–C21–C22	122.1(2)

The nonequivalence of the *o*-methyl substituents in the ^{1}H NMR spectrum for both compounds showed the absence of free rotation of the Mes groups around the Mes—C bond.

The structure of 7 is shown in Figure 3, and selected structural parameters are listed in Table IX. Vanadium is surrounded by two η^2(C,N)-bonded ligands from the original complex, an oxo oxygen atom, and an acetato group, which behaves as an unsymmetrical chelating ligand through its oxygen atoms (V–O2, 2.048(4) Å; V–O3; 2.384(4) Å). The coordination geometry can be assumed as either a trigonal or a pentagonal distorted bipyramid, the equatorial plane being defined by the N1–C10,N2–C30 η^2-bonded atoms and the O2 oxygen atoms from the acetato group. Vanadium lies 0.432(1) Å from the mean plane through these atoms, which show a maximum displacement of 0.070(5) Å for C30. The O1 oxo oxygen atom and the other oxygen from the acetato group (O3) occupy the apical positions. The unsymmetrical behavior of the acetato group is therefore a consequence of the trans effect exerted

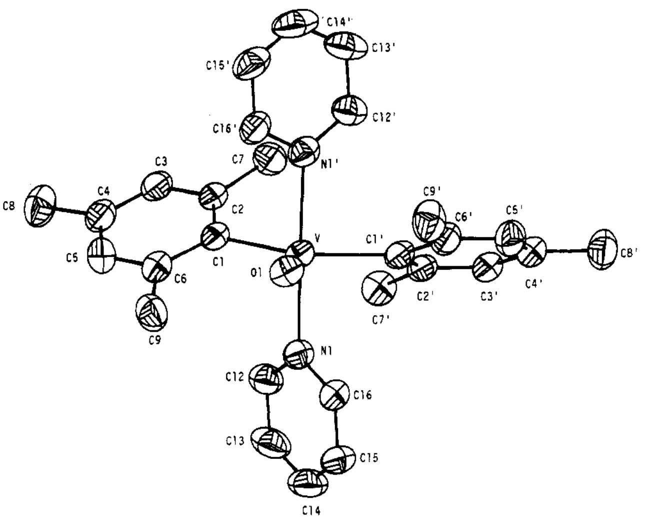

Figure 2. ORTEP view of complex 4 (30% probability ellipsoids).

Table VIII. Selected Bond Distances (Å) and Angles (deg) for Complex 4

V–O1	1.593(8)	N1–C16	1.358(10)
V–N1	2.185(6)	C1–C2	1.404(11)
V–C1	2.141(7)	C1–C6	1.419(10)
N1–C12	1.359(10)		
C1–V–C1′[a]	133.9(3)	V–N1–C16	115.2(4)
N1–V–C1′	86.8(3)	V–N1–C12	126.5(5)
N1–V–C1	90.4(3)	C12–N1–C16	118.3(6)
N1–V–N1′	172.8(3)	V–C1–C6	120.5(5)
O1–V–C1	113.1(2)	V–C1–C2	122.9(5)
O1–V–N1	93.6(2)	C2–C1–C6	116.6(6)

[a] The prime indicates the symmetry transformation $1 - x, y, 1.5 - z$.

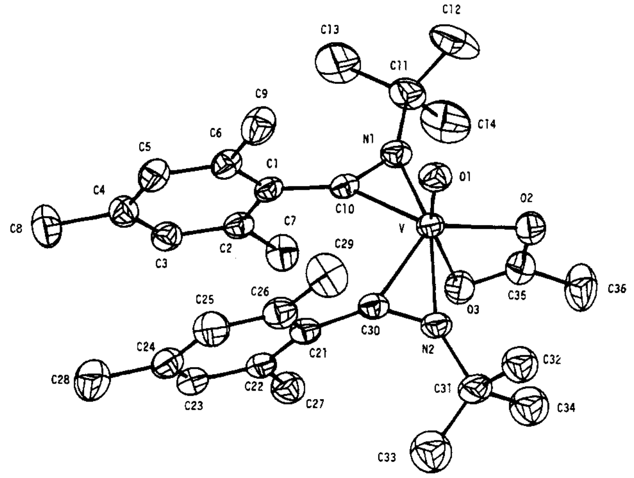

Figure 3. ORTEP view of complex 7 (30% probability ellipsoids).

Table IX. Selected Bond Distances (Å) and Angles (deg) for Complex 7

V–O1	1.594(4)	O3–C35	1.255(7)
V–O2	2.048(4)	N1–C10	1.238(5)
V–O3	2.384(4)	N1–C11	1.487(5)
V–N1	2.044(4)	N2–C30	1.248(7)
V–N2	2.041(4)	N2–C31	1.492(8)
V–C10	2.030(4)	C1–C10	1.462(5)
V–C30	2.028(4)	C21–C30	1.456(5)
O2–C35	1.271(7)		
C10–V–C30	91.3(2)	O1–V–N1	101.1(2)
N2–V–C30	35.7(2)	O1–V–O3	162.5(2)
N2–V–C10	123.7(2)	O1–V–O2	104.1(2)
N1–V–C30	125.9(2)	V–O2–C35	98.4(3)
N1–V–C10	35.4(1)	V–O3–C35	83.4(3)
N1–V–N2	151.9(2)	V–N1–C11	152.2(3)
O3–V–C30	94.0(1)	V–N1–C10	71.7(3)
O3–V–C10	88.9(1)	C10–N1–C11	135.7(4)
O3–V–N2	80.8(1)	V–N2–C31	153.0(3)
O3–V–N1	80.4(1)	V–N2–C30	71.6(3)
O2–V–C30	127.9(2)	C30–N2–C31	135.3(4)
O2–V–C10	127.0(2)	N1–C10–C1	139.6(4)
O2–V–N2	93.2(2)	V–C10–C1	147.4(3)
O2–V–N1	94.5(2)	V–C10–N1	72.9(3)
O2–V–O3	58.4(1)	N2–C30–C21	140.1(4)
O1–V–C30	98.9(2)	V–C30–C21	147.0(3)
O1–V–C10	102.5(2)	V–C30–N2	72.7(3)
O1–V–N2	103.1(2)	O2–C35–O3	119.6(5)

Scheme I

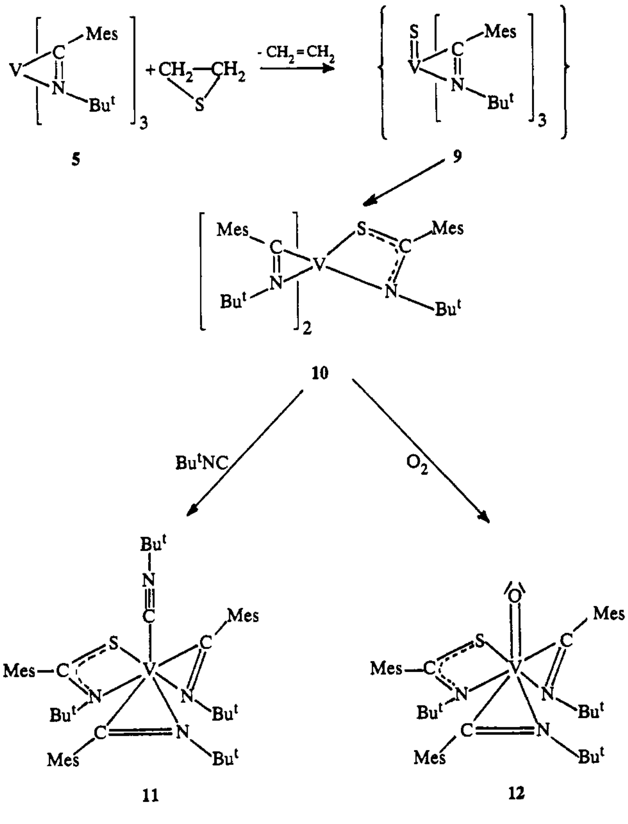

by the multiple V–O1 bond on the V–O3 bond. All the other distances fall in the normal range. Vanadium does not lie exactly on the acetato plane, being displaced by 0.098(1) Å. The C1⋯C16 and C21⋯C26 aromatic rings are nearly parallel to each other (dihedral angle 13.1(1)°) and are nearly parallel to the V,O2,O3,C35,C36 mean plane (dihedral angles 5.4(2) and 15.7(1)°, respectively), so that all these groups are nearly perpendicular to the equatorial coordination plane (dihedral angles 84.7(1), 78.8(1), and 89.2(1)°, respectively).

In an attempt to produce the thio equivalent of **6** we used a thioepoxide, instead of an epoxide, in Scheme I. The final product forming from the reaction is **10**, rather than **9**.

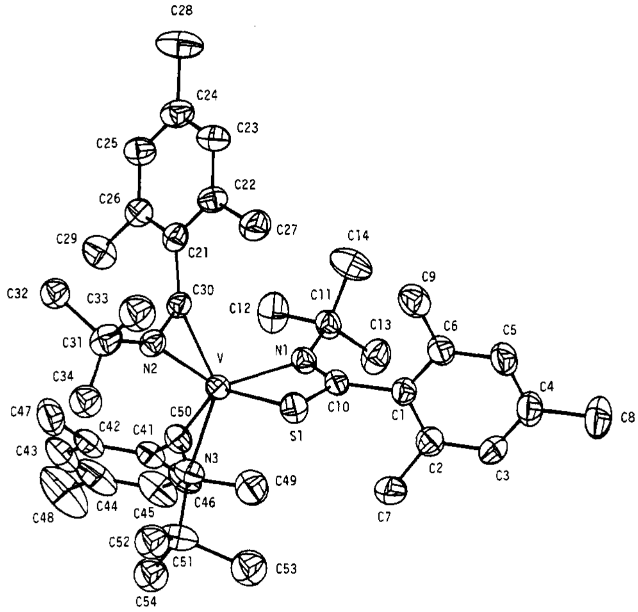

Figure 4. ORTEP view of complex **10** (30% probability ellipsoids).

Table X. Selected Bond Distances (Å) and Angles (deg) for Complex 10

V–S1	2.464(3)	N1–C11	1.517(9)
V–N1	2.076(6)	N2–C30	1.243(9)
V–N2	2.013(6)	N2–C31	1.520(11)
V–N3	2.013(7)	N3–C50	1.277(9)
V–C30	2.038(8)	N3–C51	1.508(12)
V–C50	2.058(9)	C1–C10	1.497(8)
S1–C10	1.733(7)	C21–C30	1.495(9)
N1–C10	1.300(9)	C41–C50	1.487(10)
C30–V–C50	115.6(3)	V–N1–C10	101.0(5)
N3–V–C50	36.5(3)	C10–N1–C11	125.9(6)
N3–V–C30	137.0(3)	V–N2–C31	151.8(5)
N2–V–C50	109.6(3)	V–N2–C30	73.2(4)
N2–V–C30	35.7(3)	C30–N2–C31	134.1(7)
N2–V–N3	110.0(3)	V–N3–C51	152.0(6)
N1–V–C50	110.2(3)	V–N3–C50	73.6(4)
N1–V–C30	99.9(3)	C50–N3–C51	134.3(7)
N1–V–N3	119.1(3)	N1–C10–C1	129.2(6)
N1–V–N2	130.8(3)	S1–C10–C1	116.9(5)
S1–V–C50	134.1(2)	S1–C10–N1	113.8(5)
S1–V–C30	109.6(2)	N2–C30–C21	134.6(6)
S1–V–N3	101.7(2)	V–C30–C21	153.9(5)
S1–V–N2	102.1(2)	V–C30–N2	71.1(4)
S1–V–N1	67.8(2)	N3–C50–C41	130.4(6)
V–S1–C10	76.1(2)	V–C50–C41	159.8(5)
V–N1–C11	133.2(5)	V–C50–N3	69.8(5)

We propose **9**, the thio analogue of **6**, as an intermediate in the formation of **10**. A migration of one carbon produces a thioamido ligand and corresponds to an internal reductive elimination. Complex **10** is a vanadium(III) derivative having a μ_{eff} value of 2.60 μ_B at 293 K.

The structure of **10** is reported in Figure 4, and selected structural data are given in Table X. The insertion of the sulfur atom into the V–C bond of **5** does not much affect the geometry of the V(MesCNBu^t)$_2$ residue as far as bond distances, bond angles, and the mutual orientation of the two systems of η^2-bonded V,N,C atoms (dihedral angles 73.6(4)°) are concerned.[13] The mesityl rings still remain nearly perpendicular to the V,N,C planes (dihedral angles: V,N2,C30 ∧ C21⋯C26 = 88.3(3)°; V,N3,C50 ∧ C41⋯C46 = 84.3(4)°). The sulfur-containing ligand behaves as a chelating ring through the sulfur and nitrogen atoms, giving rise to a four-membered chelation ring which is not planar, vanadium being displaced by 0.408(1) Å from the S1,C10,N1 plane. The S1–C10 (1.733(7) Å) and N1–C10 (1.300(9) Å) bond distances have a considerable double-bond character, indicating a π delocalization. The C1···C6 mesityl ring is nearly perpendicular to the S1,C10,N1 plane, the dihedral angle they form being 81.5(2)°. The chemistry of **10** is related to the chemical behavior of other vanadium(III) derivatives reported in this or the preceding paper.[13] Complex **10** binds π-acids to give **11**, for example, and **15**, oxidized by molecular oxygen to the corresponding oxovanadium(V) species **12**. The ^{1}H NMR spectrum of **12** shows the presence of three different mesityl groups, suggesting the presence of two geometrically nonequivalent η^2-iminoacyls, as in the proposed structure.

Though the reaction of organometallic and coordination compounds of vanadium(III) with molecular oxygen is in general complex and synthetically useless,[5,17] this was not the case for the reaction reported in Scheme I and eq 6.

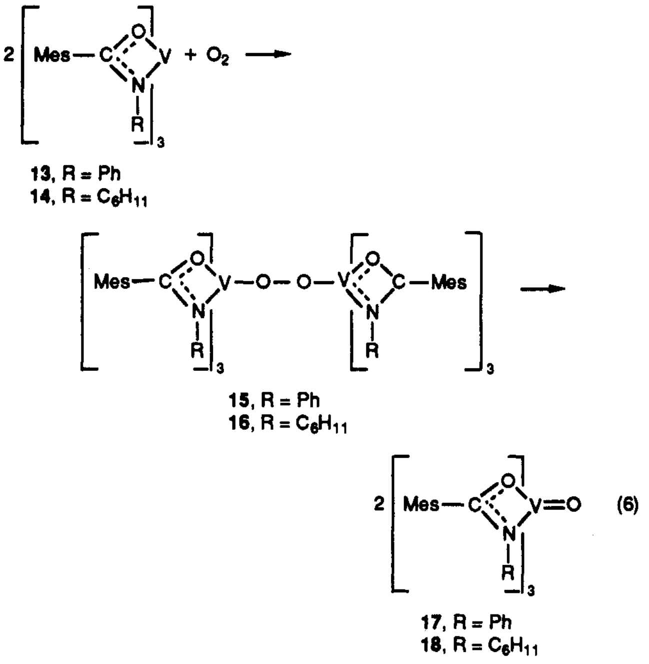

13, R = Ph
14, R = C_6H_{11}

15, R = Ph
16, R = C_6H_{11}

17, R = Ph
18, R = C_6H_{11}

The amount of oxygen absorbed during the reaction corresponded to a V:O_2 ratio of 2:1. Reaction 6 is clean, and the yield is over 80%. This allows us to suggest the intermediacy of μ-peroxo complexes **15** and **16**, which evolve to the oxovanadium(V) complexes **17** and **18**. The reaction with O_2 was followed by a continuous cryoscopic measurement of the molecular weight, but only a monomeric form was observed. This may be the consequence of a very fast decomposition of the peroxo to the oxo species. Although the reaction was carried out at low temperatures, we were unable to identify any of the proposed peroxo intermediates.

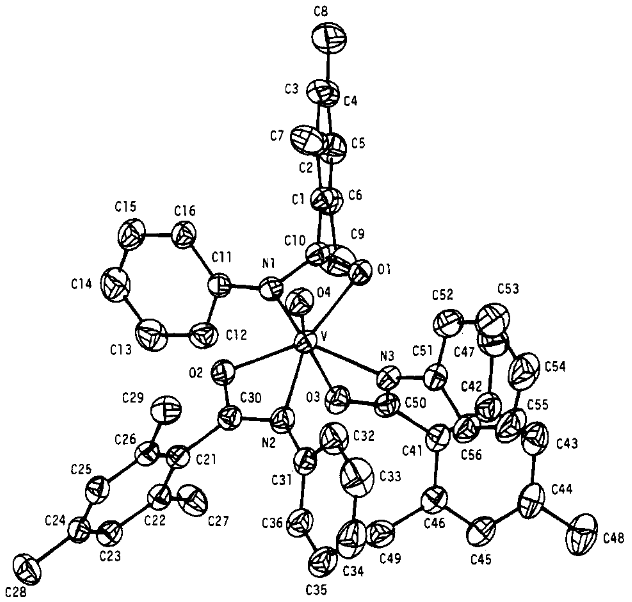

Figure 5. ORTEP view of complex **17** (30% probability ellipsoids).

Table XI. Selected Bond Distances (Å) and Angles (deg) for Complex 17

V–O1	2.152(3)	N1–C10	1.314(5)
V–O2	2.010(3)	N1–C11	1.406(4)
V–O3	2.197(3)	N2–C30	1.283(5)
V–O4	1.593(3)	N2–C31	1.420(4)
V–N1	2.053(3)	N3–C50	1.318(5)
V–N2	2.112(3)	N3–C51	1.412(4)
V–N3	2.041(3)	C1–C10	1.474(5)
O1–C10	1.284(4)	C21–C30	1.489(5)
O2–C30	1.308(5)	C41–C50	1.493(5)
O3–C50	1.275(5)		
N2–V–N3	81.2(1)	V–O1–C10	91.5(2)
N1–V–N3	129.6(1)	V–O2–C30	95.3(2)
N1–V–N2	138.3(1)	V–O3–C50	89.5(2)
O4–V–N3	103.7(1)	V–N1–C11	138.0(2)
O4–V–N2	92.3(1)	V–N1–C10	95.1(2)
O4–V–N1	103.8(1)	C10–N1–C11	126.9(3)
O3–V–N3	61.4(1)	V–N2–C31	141.8(2)
O3–V–N2	86.7(1)	V–N2–C30	91.4(2)
O3–V–N1	86.5(1)	C30–N2–C31	126.5(3)
O3–V–O4	165.1(1)	V–N3–C51	136.9(2)
O2–V–N3	135.9(1)	V–N3–C50	95.4(2)
O2–V–N2	62.3(1)	C50–N3–C51	127.7(3)
O2–V–N1	76.7(1)	N1–C10–C1	126.0(3)
O2–V–O4	101.7(1)	O1–C10–C1	122.3(3)
O2–V–O3	91.0(1)	O1–C10–N1	111.6(3)
O1–V–N3	78.4(1)	N2–C30–C21	130.6(3)
O1–V–N2	159.0(1)	O2–C30–C21	118.5(3)
O1–V–N1	61.4(1)	O2–C30–N2	110.0(3)
O1–V–O4	87.9(1)	N3–C50–C41	125.1(3)
O1–V–O3	87.8(1)	O3–C50–C41	121.3(3)
O1–V–O2	138.1(1)	O3–C50–N3	113.5(3)

The structure of **17** is shown in Figure 5. Table XI contains a selected list of structural parameters. Coordination could be considered as a pentagonal bipyramid, with the O1,N1,O2,N2,N3 atoms defining the equatorial plane and the O3,O4 atoms occupying the apices. However, the increased oxidation number of vanadium and the presence of a V–O4 multiple bond cause significant differences. In particular, the V–N bond distances (2.053(3), 2.112(3), 2.041(3) Å) are significantly shorter than those found in [V{O—C(Mes)=NPh}$_3$(py)] (2.162(3), 2.102(3), 2.188(3) Å); the V—O single-bond distances fall in a wider range, the longer value (2.197(3) Å) being observed for the V–O3 distance trans to the multiple V=O4 bond. The observed difference could also be related to different intraligand steric interactions due to the interchange between oxygen and nitrogen at coordination sites occupied by the ligand perpendicular to the coordination plane. In the present compound the nitrogen atom (N3) is in the equatorial plane and the oxygen atom (O3) is in the axial position, while in [V{O-C(Mes)=NPh}$_3$(py)] they are interchanged.

The reaction of **17** with its vanadium(III) precursor **13** led to the formation of a bridging oxovanadium(IV) dimer in the form of red crystals:

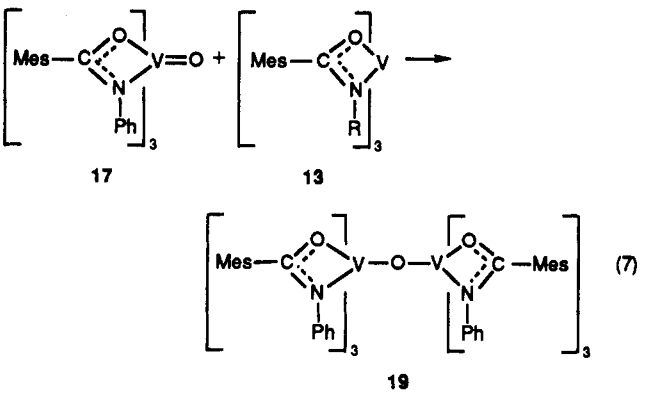

Complex **19** has been fully characterized as reported in the Experimental Section; however, an X-ray analysis could not be performed.

Experimental Section

General Procedure. All reactions were carried out under an atmosphere of purified nitrogen. Solvents were dried and distilled before use by standard methods. [V(Mes$_3$)·THF], [V{η^2-C(Mes)═NBu^t}$_3$], and [V{O—C(Mes)═NR}$_3$] (R = C_6H_{11}, Ph) have been prepared as reported.[13] Infrared spectra were recorded with a Perkin-Elmer 883 spectrophotometer; NMR spectra were measured on a Bruker 200-AC instrument. The magnetic measurements were made using a Faraday balance.

Reaction of [V(Mes)$_3$·THF] (1) with Epoxides: Synthesis of 2. To a THF (100 mL) solution of **1** (2.717 g, 5.66 mmol) was added Ph—HC═CH$_2$—O (0.65 mL, 5.69 mmol), and the color suddenly changed from blue to orange. The solution was stirred for 30 min and then concentrated to dryness and the residue extracted with *n*-hexane (100 mL). The orange solution obtained was filtered and concentrated, yielding orange crystals of the product (2.0 g, 83%). Anal. Calcd for $C_{27}H_{33}OV$: C, 76.40; H, 7.84. Found: C, 76.69; H, 8.27. MW (cryoscopy in benzene): found, 396; required, 424. ^{1}H NMR (C_6D_6): δ 6.94 (s, 2 H, H Mes), 2.74 (s, 3 H, o-Me Mes), 1.98 (s, 3 H, *p*-Me Mes). We did not observe any temperature dependence of the ^{1}H NMR spectrum. [O═V(Mes)$_3$] is thermally very stable, a very slight decomposition being observed after 17 h of reflux in THF. It decomposes very slowly in air both in solution and in the solid state. ν(V═O) (Nujol): 1029 cm^{-1}. **2** is obtained from **1** by using other epoxides, the only difference being the reaction time. A much slower reaction was observed when O—CH$_2$—CH—CH$_2$-CH$_3$ was employed. The reaction of **1** with dry O_2 in *n*-hexane gave a deep red solution, from which we have been unable to identify clean compounds.

Reaction of 1 with 2: Synthesis of 3. Compound **1** (1.64 g, 3.41 mmol) was added to a solution of **2** (1.45 g, 3.41 mmol) in toluene (125 mL). The solution suddenly became red. It was stirred for 30 min and then concentrated to 50 mL. A red crystalline product was obtained (2.158 g, 76%). Anal. Calcd for $C_{54}H_{66}OV_2$: C, 77.86; H, 7.99. Found: C, 77.49; H, 8.16. μ_{eff}: 1.81 μ_B at 293 K. ν(V-O-V) (Nujol): 680 cm^{-1}. Attempts to crystallize the μ-oxo complex from polar solvents such as THF were unsuccessful due to the induced partial decomposition caused by the solvent, as shown by the reaction of **3** with pyridine.

Reaction of 3 with Pyridine: Synthesis of 4. To a THF (100 mL) solution of pyridine (0.3 mL, 3.72 mmol) was added (Mes)$_3$VOV(Mes)$_3$ (0.76 g, 0.91 mmol). A green solution was obtained, which was stirred for 6 h at room temperature and then concentrated to ca. 10 mL. Upon addition of *n*-hexane (90 mL) and cooling, crystals of the product were obtained (0.39 g, 46%). The major product is mixed with a small amount of byproduct, which very often affects the microanalysis. ν(V═O) (Nujol): 1012 cm^{-1}. μ_{eff}: 1.65 μ_B at 288 K.

Reaction of 5 with Epoxides: Synthesis of 6. A THF (100 mL) solution of **5** (2.1 g, 3.19 mmol) was reacted with Ph—CH—CH$_2$—O (0.37 g, 3.24 mmol) at 0 °C and the color suddenly turned orange-yellow. The solution was allowed to react for 30 min and then concentrated to dryness and the residue washed with *n*-hexane (25 mL). A yellow solid was obtained (diamagnetic; 1.61 g, 75%). Anal. Calcd for $C_{42}H_{60}N_3OV$: C, 74.86; H, 8.97; N, 6.23. Found: C, 74.84; H, 8.94; N, 5.93. ν(V═O) (Nujol): 946 cm^{-1}. ν(C═N) (Nujol): 1678 cm^{-1}. The oxovanadium(V) complex is thermally labile, decomposing in 15 min in solution at room temperature. All the solutions have to be handled at 0 °C or lower. ^{1}H NMR (CDCl$_3$, 20 °C): δ 6.68 (s, 2 H, H Mes), 2.31 (s, 3 H, *p*-Me Mes), 2.19 (s, 6 H, *o*-Me Mes), 1.27 (s, 9 H, Bu^t). ^{1}H NMR (CDCl$_3$, -40 °C): δ 6.97 (s, 2 H, H Mes), 6.56 (s, 2 H, H Mes), 6.53 (s, 2 H, H Mes), 2.68 (s, 6 H, *o*-Me Mes), 2.40 (s, 3 H, *p*-Me Mes), 2.30 (s, 6 H, *p*-Me Mes), 2.08 (s, 6 H, *o*-Me Mes), 1.85 (s, 6 H, *o*-Me Mes), 1.29 (s, 18 H, Bu^t), 1.11 (s, 9 H, Bu^t). ^{13}C NMR (CDCl$_3$, -40 °C): δ 217.95 (1C, MesC═NBu^t), 208.22 (2C, MesC═NBu^t).

Reaction of 6 with Acetic Acid: Synthesis of 7. To a THF (75 mL) solution of CH$_3$COOH (0.08 mL, 140 mmol), **6** (0.914 g, 1.36 mmol) was added and the color immediately turned pale yellow. The solution was stirred for 30 min at room temperature; then the solvent was evaporated to dryness. The residue was dissolved in *n*-hexane (50 mL) and filtered. Upon concentration, pale yellow crystals formed (0.61 g, 85%). Anal. Calcd for $C_{30}H_{43}N_2O_3V$: C, 67.91; H, 8.17; N, 5.28. Found: C, 67.83; H, 8.00; N, 5.39. ν(V═O) (Nujol): 975 cm^{-1}. ν(C═N) (Nujol): 1558 cm^{-1}. ν(CO$_2$) (Nujol): 1722 cm^{-1}. ^{1}H NMR (C_6D_6, 20 °C): δ 6.46 (s, 2 H, H Mes), 6.42 (s, 2 H, H Mes), 2.24 (s, 6 H, Me Mes), 2.02 (s, 3 H, CH$_3$CO$_2$), 2.00 (s, 6 H, Me Mes), 1.82 (s, 6 H, Me Mes), 1.46 (s, 18 H, Bu^t). ^{13}C NMR (CDCl$_3$, 20 °C): δ 203.53 (MesC*═NBu^t).

Reaction of 6 with HCl: Synthesis of 8. At room temperature, a yellow THF (75 mL) solution of **6** (0.571 g, 0.85 mmol) was added to an aqueous solution of HCl (0.11 mL, 8.56 M, 0.94 mmol). The color immediately turned pale yellow. The solution was stirred for 15 min at room temperature and then concentrated to 20 mL. *n*-Hexane (10 mL) was added. When it was cooled, the filtered solution yielded yellow crystals (0.36 g, 84%). Anal. Calcd for $C_{28}H_{40}ClN_2OV$: C, 66.33; H, 7.95; N, 5.52. Found: C, 66.58; H, 8.09; N, 5.52. ν(V═O): 996 cm^{-1}. ν(C═N) (Nujol): 1716 (s) and 1734 (m) cm^{-1}. ^{1}H NMR (CDCl$_3$, 20 °C): δ 6.64 (s, 1 H, H Mes), 6.57 (s, 1 H, H Mes), 2.24 (s, 3 H, H Mes), 2.09 (s, 3 H, Me Mes), 1.68 (s, 9 H, Bu^t), 1.57 (s, 3 H, Me Mes). ^{13}C NMR (CDCl$_3$, +20 °C): δ 203.73 (MesC*═NBu^t).

Reaction of 5 with Ethylene Sulfide: Synthesis of 10. CH$_2$—CH$_2$—S (0.25 mL, 4.2 mmol) was added to a THF (100 mL) solution of **5** (2.77 g, 4.21 mmol). The color immediately turned red. The solution was stirred for 30 min at room temperature, then the solvent evaporated to dryness. The red residue was dissolved in *n*-hexane (125 mL) and filtered. Concentration of the solution gave red crystals of [V{η^2-C(Mes)═NBu^t}$_2${SC(Mes)═NBu^t}]·C_6H_{14} (2.42 g, 74%). Anal. Calcd for $C_{42}H_{60}N_3SV{\cdot}C_6H_{14}$: C, 74.48; H, 9.37; N, 5.43. Found: C, 74.28; H, 9.47; N, 5.74. μ_{eff}: 2.60 μ_B at 293 K. ν(C═N): 1550 and 1570 cm^{-1}.

Reaction of 10 with CNBu^t: Synthesis of 11. A THF (100 mL) solution of [V{η^2-C(Mes)═NBu^t}$_2${SC(Mes)═NBu^t}]·C_6H_{14} (1.04 g, 1.34 mmol) was reacted with CNBu^t (0.17 mL, 1.50 mmol). After 2 h of stirring at room temperature, the solvent was evaporated to dryness and the residue washed with *n*-hexane (20 mL). A yellow-green solid was obtained (0.65 g, 63%). Anal. Calcd for $C_{47}H_{69}N_4SV$: C, 73.02; H, 9.00; N, 7.25. Found: C, 73.11; H, 9.21; N, 6.66. μ_{eff}: 257 μ_B at 293 K. ν(C═N) (Nujol): 1643 cm^{-1}. ν(C≡N) (Nujol): 2135 cm^{-1}.

Reaction of 10 with Dioxygen: Synthesis of 12. An *n*-hexane (100 mL) solution of [V{η^2-C(Mes)═NBu^t}$_2${SC(Mes)═NBu^t}]·C_6H_{14} (1.10 g, 1.42 mmol) was reacted with an excess of molecular oxygen. The solution became yellow and a large amount of a yellow solid crystallized (0.63 g, 63%). Anal. Calcd for $C_{42}H_{60}N_3OSV$: C, 71.46; H, 8.57; N, 5.95. Found: C, 71.39; H, 8.66; N, 5.51. ν(V=O) (Nujol): 946 cm^{-1}. ν(C=N) (Nujol): 1729 cm^{-1}. ^{1}H NMR (C_6D_6, 20 °C): δ 6.73 (s, 2 H, H Mes), 6.46 (s, 4 H, H Mes), 2.58 (s, 6 H, H Mes), 2.24 (s, 6 H, Me Mes), 2.14 (s, 9 H, H Mes), 1.96 (s, 6 H, Me Mes), 1.57 (s, 18 H, Bu^t), 0.96 (s, 9 H, Bu^t). ^{13}C NMR ($CDCl_3$): δ 163.07 (1C, CH=N), 197.99 (2C, CH=N).

Reaction of 13 with Dioxygen: Synthesis of 17. A THF (100 mL) solution of [V{O—C(Mes)=NPh}$_3$] (4.5 g, 5.88 mmol) was treated with dry oxygen in excess at room temperature for 30 min. A dark red solution was obtained, which was evaporated to dryness and extracted with diethyl ether in an extractor filter. A red crystalline product was obtained (3.7 g, 80%). Anal. Calcd for $C_{48}H_{48}N_3O_4V$: C, 73.74; H, 6.19; N, 5.37. Found: C, 73.66; H, 6.50; N, 5.48. ν(V=O) (Nujol): 976 cm^{-1}. ν(CNO) (Nujol): 1553 and 1594 cm^{-1}. The oxygen uptake corresponded to a 2:0.97 V:O_2 molar ratio. The reaction with O_2 was followed by continuous cryoscopic measurements of the molecular weight. Only a monomeric form was observed. ^{1}H NMR (C_6D_6, 20 °C): δ 7.29 (d, 2 H, Ph), 6.87 (t, 2 H, Ph), 6.73 (t, 1 H, Ph), 6.44 (s, 2 H, H Mes), 2.41 (s, 6 H, *o*-Me Mes), 1.90 (s, 3 H, *p*-Me Mes). ^{13}C NMR ($CDCl_3$): δ 163.07 (1C, CH=N), 197.99 (2C, CH=N).

Reaction of 14 with Dioxygen: Synthesis of 18. To a green THF (100 mL) solution of **14** (2.96 g, 3.77 mmol) dry oxygen was added in excess. Suddenly the color changed to red. The solution was stirred for 30 min at room temperature; then the solvent was evaporated to dryness and the residue redissolved in *n*-hexane (75 mL). The solution was filtered and concentrated and a red crystalline product was obtained (2.63 g, 83%). Anal. Calcd for $C_{48}H_{66}N_3O_4V$: C, 72.07; H, 8.32; N, 5.25. Found: C, 71.98; H, 8.24; N, 5.21. ν(V=O) (Nujol): 984 cm^{-1}. ν(CNO) (Nujol): 1648, 1586, 1550 cm^{-1}. ^{1}H NMR (C_6D_6, 20 °C): δ 6.66 (s, 2 H, H Mes), 3.35 (m, 1 H, Cy), 2.47 (s, 6 H, *o*-Me Mes), 2.03 (s, 3 H, *p*-Me Mes), 2.16–0.97 (m, 10 H, Cy). The oxygen uptake corresponded to a 2:0.98 V:O_2 molar ratio.

Synthesis of 19. To a THF (50 mL) solution of **13** (0.88 g, 1.15 mmol) was added a THF (50 mL) solution of **17** (0.9 g, 1.15 mmol). The mixture was allowed to react for 24 h; then *n*-hexane (40 mL) was added. Upon concentration, a red crystalline solid formed (1.17 g, 65%). Anal. Calcd for $C_{96}H_{96}N_6O_7V_2$: C, 74.50; H, 6.25; N, 5.43. Found: C, 74.09; H, 7.05; N, 4.94. μ_{eff}: 1.29 μ_B at 293 K. ν(V–O–V) (Nujol): 700 cm^{-1}. ν(C=N) (Nujol): 1580 cm^{-1}. The μ-oxo compound is significantly less soluble than the oxovanadium(V) precursor. It can be crystallized from THF.

Crystal Structure Determination of Complexes 2, 4, 7, 10, and 17. The crystals selected for study were mounted in glass capillaries and sealed under nitrogen. The reduced cells were obtained with use of TRACER.[18] Crystal data and details associated with data collection are given in Table I. For intensity background, individual reflection profiles were analyzed.[19] The structure amplitudes were obtained after the usual Lorentz and polarization corrections,[20] and the absolute scale was established by the Wilson method.[21] Data for complexes 7, 10, and 17 were corrected for absorption using ABSORB.[22] The function minimized during the full-matrix least-squares refinement was $\sum w|\Delta F|^2$. A weighting scheme based on counting statistics[20] was applied for complexes 2 and 17, while unit weights were used for complexes 4, 7, and 10 resulting in more satisfactory agreement analysis. Scattering factors for neutral atoms were taken from ref 23a for non-hydrogen atoms and from ref 24 for H. Anomalous scattering corrections were included in all structure factor calculations.[23b] Among the low-angle reflections no correction for secondary extinction was deemed necessary.

Solution and refinement were based on the observed reflections. All the structures were solved by direct methods using SHELX-86.[25]

Complex 2. Refinement was first done isotropically and then anisotropically for all the non-H atoms. The hydrogen atoms were located from a difference Fourier map and introduced as fixed contributors (U_{iso} = 0.08 Å^2).

Complex 4. Refinement was first done isotropically and then anisotropically for all the non-H atoms of the complex molecule. X-ray analysis revealed three independent peaks distributed around a center of symmetry which were isotropically refined with site occupation factors of 0.5. They were interpreted as a pyridine molecule of crystallization generated by the center of symmetry in a complex:pyridine ratio of 2:1. Owing to the high thermal motion affecting these atoms, it was not possible to distinguish between nitrogen and carbon atoms. The associated hydrogen atoms were ignored, while all the others were located in a difference Fourier map and introduced prior to the final refinement as fixed contributors (U_{iso} = 0.08 Å^2). Because of the rather high absorption coefficient an empirical absorption correction was applied[22] and the structure refined to convergence again. The refinement resulted in final *R* values significantly higher than those corresponding to the original set (R = 0.058, R_G = 0.157 vs R = 0.111, R_G = 0.157 ($R_G = [\sum w^{1/2}|\Delta F|^2/\sum w^{1/2}|F_o|^2]^{1/2}$)), and it was discarded. Final coordinates quoted in Table III refer to the data not corrected for absorption.

Complex 10. Refinement was first done isotropically and then anisotropically for all the non-H atoms with the exception of the C32, C33, and C34 methyl carbon atoms. These were found to be statistically distributed over two positions and isotropically refined with site occupation factors given in Table IV. The hydrogen atoms were located from a difference Fourier map and introduced as fixed contributors (U_{iso} = 0.08 Å^2).

Complex 17. Refinement was first done isotropically and then anisotropically for all the non-H atoms. The hydrogen atoms were located from a difference Fourier map and introduced as fixed contributors (U_{iso} = 0.08 Å^2).

During the refinements all the mesityl and phenyl rings in complexes 2, 7, 10, and 17 were constrained to be regular hexagons (C–C = 1.395 Å). In the final cycle of refinements no parameter shifted by more than 0.2 times its standard deviation. The final difference maps showed no unusual features, with no significant peak above the general background.

Final atomic coordinates are listed in Tables II–VI for non-H atoms and in Tables SI–SV for hydrogens. Thermal parameters are given in Tables SVI–SX[26] and selected interatomic distances and angles in Tables VII–XI.

Acknowledgment. We thank the "Fonds National Suisse de la Recherche Scientifique" (Grant No. 20-28470-90), the "Fondation Herbette" (University of Lausanne), and the U.S. Navy (Grant No. N00014-89-J-1810) for financial support.

Supplementary Material Available: Listings of unrefined hydrogen coordinates (Tables SI–SV), thermal parameters (Tables SVI–SX), and bond distances and angles (Tables SXI–SXV) for 2, 4, 7, 10, and 17 (16 pages). Ordering information is given on any current masthead page.

OM920619C

---

(18) Lawton, S. L.; Jacobson, R. A. TRACER, a Cell Reduction Program; Ames Laboratory, Iowa State University of Science and Technology: Ames, IA, 1965.

(19) Lehmann, M. S.; Larsen, F. K. *Acta Crystallogr.* **1974**, *A30*, 580.

(20) Data reduction, structure solution, and refinement were carried out on a Gould 32/77 computer using: Sheldrick, G. SHELX-76 System of Crystallographic Computer Programs; University of Cambridge: Cambridge, England, 1976.

(21) Wilson, A. J. C. *Nature (London)* **1942**, *150*, 151.

(22) Uguzzoli, F. ABSORB, a Program for F_o Absorption Correction; University of Parma: Parma, Italy, 1985 (following: Walker, N.; Stewart, D. *Acta Crystallogr., Sect. A* **1983**, *A39*, 158).

(23) (a) *International Tables for X-ray Crystallography*; Kynoch Press: Birmingham, England, 1974; Vol. IV, p 99. (b) *Ibid.*, p 149.

(24) Stewart, R. F.; Davidson, E. R.; Simpson, W. T. *J. Chem. Phys.* **1965**, *42*, 3175.

(25) Sheldrick, G. SHELX-86, a FORTRAN-77 Program for the Solution of Crystal Structure from Diffraction Data; University of Cambridge: Cambridge, England, 1986.

(26) See paragraph at the end of the paper regarding supplementary material.